Porous Media Compressed Air Energy Storage (PM-CAES):

Theory and Simulation of the Coupled Wellbore-Reservoir System

Curtis M. Oldenburg and Lehua Pan

Earth Sciences Division 90-1116
Lawrence Berkeley National Laboratory
Berkeley, CA 94720

Corresponding author:
cmoldenburg@lbl.gov
510-486-7419

Keywords: Compressed Air Energy Storage, CAES, Aquifer CAES, wellbore flow

Abstract

Expansion in the supply of intermittent renewable energy sources on the electricity grid can potentially benefit from implementation of large-scale compressed air energy storage in porous media systems (PM-CAES) such as aquifers and depleted hydrocarbon reservoirs. Despite a large government research program 30 years ago that included a test of air injection and production in an aquifer, and an abundance of literature on CAES mostly relevant to caverns, there remain fundamental questions about the hydrologic and energetic performance of PM-CAES. We have developed rigorous simulation capabilities for PM-CAES that include modeling the coupled wellbore-reservoir system. Through consideration of a prototypical PM-CAES wellbore-reservoir system representing a depleted hydrocarbon reservoir, we have simulated 100 daily cycles of PM-CAES. We find that (1) PM-CAES can store energy but that pervasive pressure gradients in PM-CAES result in spatially variable energy storage density in the reservoir, (2) the wellbore-reservoir storage component of PM-CAES is very efficient, (3) cap-rock and hydrologic seals along with proper sizing of the PM-CAES reservoir prevent excess pressure diffusion from being a problem, and (4) injection and production of air does not significantly mobilize residual liquid water in the reservoir.

Introduction

Reducing greenhouse gas emissions through greater use of intermittent renewables such as wind and solar energy requires expanding the capacity of grid-scale energy storage. The largest sources of grid-scale electrical energy storage today are pumped hydro storage (PHS) at 127 GW and compressed air energy storage (CAES) at 400 MW, with PHS providing over 99% of all electrical energy storage (EPRI 2008). The small fraction of grid-scale energy storage provided by CAES is not a result of any physical or environmental limitations, but rather results from a lack of policy and economic drivers for energy storage in general and CAES in particular. The two existing CAES plants utilize solution-mined salt caverns and work on a daily cycle in an arbitrage mode providing power to meet peak demand rather than to store energy produced by renewables (Raju and Khaitan 2012).

Assuming it will someday be economically attractive to develop a large number of CAES plants to support grid-scale energy storage needs of intermittent renewable energy sources, there may be limitations in the number of salt-dome and bedded-salt sites to support salt-cavern CAES. However, it is widely accepted that there is enormous opportunity to advance CAES technology beyond caverns and use instead the pore space in aquifers and depleted hydrocarbon reservoirs as the storage volume. We refer to these options as porous media CAES or PM-CAES.

The energy storage part of CAES in general can be distilled into two simple processes: (1) injecting compressed air into a container for storage, and (2) withdrawing that compressed air at a later time to do useful work (i.e., contributing to electrical energy generation in a turbine). The use of a constant-volume cavern is an obvious way to achieve the energy storage objective. However, there is potentially much greater volume for expanding CAES capacity by including PM-CAES options. This opportunity has been recognized for decades, and CAES in subsurface aquifers has been partially tested in the past, and such projects are even the subject of a large-scale demonstration in the U.S. today (Westervelt 2010). However, there are very significant differences between storing compressed air in the pore space of geologic formations versus storing it in an open cavern. The details of the processes involved in PM-

CAES and its efficiency, as well as the challenges, have not been thoroughly studied and documented in the literature. Many fundamental questions remain.

In this paper, we will address four fundamental questions pertaining to advancing CAES beyond caverns and into porous media as follows:

1. Can pore space provide large-scale energy storage?
2. What is the efficiency of the coupled wellbore-reservoir system for storing energy?
3. Does pressure diffusivity affect storage efficiency?
4. Is energy lost due to air moving water around in the reservoir?

Without any operating examples of PM-CAES plants, the only way at present to answer these questions is through the use of numerical simulation. We have developed a rigorous coupled model of the wellbore and reservoir along with accurate equations of state approaches for modeling the fluid and energy flows in the air-water system. This approach allows us to quantify energy fluxes in the well and in the reservoir considering a wide range of physical and chemical processes. Through our simulations of a large hypothetical PM-CAES system, we will answer the four questions posed. Our work provides information useful for assessing the feasibility of developing CAES facilities in porous media in aquifers and depleted hydrocarbon reservoirs, and provides the foundation for addressing additional questions related to site-specific geologic, hydrologic, geomechanical, and geochemical (compositional) aspects of PM-CAES systems.

Prior Work

Although the use of compressed air stored in tanks for powering tools and locomotives goes back around 150 years to the latter part of the 1800's, the first subsurface grid-scale CAES plant was not operating until 1978 (Crotogino et al. 2001). This plant, the Huntorf CAES plant in Germany, which uses two solution-mined salt caverns at a depth of about 700 m to store compressed air, has been operating continuously for nearly 35 years by combining its compressed air on the energy recovery cycle with methane in a gas turbine to drive a generator to contribute 290 MW for three hours every day to meet

local peak electricity demand. The long success of the Huntorf plant is nearly matched by a similar CAES plant in McIntosh, Alabama, also making use of a solution-mined salt cavern and natural gas turbine, to provide 110 MW of peak power for several hours each day (Raju and Khaitan 2012). While the McIntosh plant improved upon the design of Huntorf by adding recuperated heat from the gas turbine to the produced compressed air, it largely employs the same approaches of Huntorf. The main salient common approaches are (1) use of a solution-mined salt cavern, and (2) multistage compression that discharges heat of compression into the atmosphere, thereby requiring fuel (natural gas) to heat the expanding air in the gas turbine in the energy recovery stage.

It was recognized in the early 1980s that research could be carried out in the area of CAES to advance it beyond its then-current state-of-the-art. This spawned a broad CAES research program in the U.S. in the 1980s funded by the U.S. Department of Energy. This effort was directed toward evaluating the potential for grid-scale CAES in several configurations including caverns in bedded and domed salt, excavated openings in hard rock environments with and without water-column pressure compensation, and in aquifers (Allen et al. 1985). All of these approaches were categorized as *conventional CAES* because they used multistage compression with heat discarded to the atmosphere, and energy recovery by feeding compressed air into a gas turbine with natural gas. This research program also included scoping and feasibility studies of *advanced CAES* approaches such as adiabatic CAES (the approach whereby heat of compression is stored as thermal energy and recovered upon production of compressed air obviating or reducing the need for natural gas), and several other exotic approaches that used alternatives to natural gas for heating the expanding air during energy recovery. The inclusion of analyses of surface infrastructure and economics made for a comprehensive research program (e.g., Schainker and Nakhamkin, 1985). Results from this U.S. DOE research program are widely reported on in conference proceedings, and summarized in Allen et al. (1985).

With cavern CAES already demonstrated at Huntorf in the late 1970's, and recognition that caverns would not perform exactly the same as aquifers, the U.S. DOE program planned and carried out an air

injection and withdrawal test in an aquifer in Pittsfield, Illinois, to test the feasibility of aquifer CAES. The results of this test are summarized in Allen et al. (1985). Briefly, the test confirmed expectations that air could be injected to create a large bubble in the aquifer, that air could be withdrawn at rates feasible for energy recovery, and that problems associated with aquifer up-coning could be avoided by proper site selection and operation. Of some surprise to the researchers were the large loss of heat to the formation through the wellbore, and the loss of oxygen in the stored air due likely to oxidation reactions with minerals in the formation. The project team concluded that wells would have to be highly insulated against thermal losses if there was any hope of recovering energy that was embodied as heat in the injected air, and that the oxidation reactions were long-time-scale processes not likely to affect air cycled on daily or weekly time frames.

With the growing concerns about greenhouse gas emissions from fossil fuel use beginning in the late 1990's, interest began to grow in large-scale deployment of renewable energy sources such as wind and solar. The intermittency of these energy sources triggered renewed interest in CAES which continues to this day. An excellent comprehensive summary and review of CAES with emphasis on its importance for wind energy was written by Succar and Williams (2008). Many of the recent publications on CAES focus on its contributions to the grid from an energy analysis perspective that assumes CAES is a developed and available storage technology (e.g., Denholm and Sioshansi 2009), while other research is taking a much more detailed look at the physics of CAES (e.g., Raju and Khaitan 2012; Kushnir et al. 2012). Other recent work on detailed process modeling is being carried out for lined rock caverns (Rutqvist et al. 2012; Kim et al. 2012).

Although significant differences exist between an open cavern and the distributed pore space in an aquifer, aquifer CAES was classified as *conventional CAES* by the researchers in the DOE program of the 1980s (Allen et al. 1985). This classification was likely in no small part due to the analogy between natural gas storage and CAES, natural gas storage having been carried out in aquifers and depleted gas reservoirs since the 1940s (Allen 1985). In fact, some of the important work in the early development of

the theoretical foundations for aquifer CAES was done by leaders in natural gas storage (e.g., Katz and Lady 1976). And hydrologists contributed to the analysis of the feasibility and design of aquifer CAES through early modeling studies (Meiri and Karadi 1982; Braester and Bear 1984) and more recent analytical solutions (Kushnir et al. 2010).

Despite the early classification of aquifer CAES (a specific type of PM-CAES) as conventional, the pioneering modeling studies of aquifer CAES, and the current large-scale projects attempting to demonstrate PM-CAES (Westervelt 2010), the fact remains that storage and recovery of compressed air through long wellbores screened in partially water-saturated and/or partially water- and hydrocarbon-saturated porous media are not well understood. Many outstanding issues remain to be addressed before PM-CAES can be considered established technology. We take the kinds of issues studied by Meiri and Karadi (1982) and Braester and Bear (1984) and Kushnir et al. (2010) involving detailed consideration of what goes on in the porous media with respect to fluid flow, heat flow, and mass transfer during CAES cycling as our point of departure from prior work. Specifically, our investigation focuses entirely on the subsurface part of the aquifer or depleted reservoir CAES system, ignores the surface infrastructure of compressors, motor-generators, and turbines, but includes detailed consideration of the well and reservoir. We use rigorous simulation tools developed on the foundation of LBNL's TOUGH2 code (Pruess et al. 1999; Pruess 2004), and we simulate the detailed processes of coupled wellbore-reservoir CAES in porous media to answer fundamental questions about energy fluxes, storage efficiency, effects of porous media, and effects of native fluids on PM-CAES. Through our work, we intend to advance the state of the art to inform the design of new and large-scale PM-CAES projects.

CAES Fundamentals

Simplified Energy Storage Equations

As useful background for understanding how CAES works, we start with the First Law of Thermodynamics for open systems (mass transfer non-zero), which says that the change in energy of a

system is equal to the heat flow in/out, the work done on/by the system, and the change in energy due to changes in kinetic energy, potential energy, and the pressure-volume work related to forcing mass into and out of the system. This change in energy for an open system can be written

$$E_2 - E_1 = Q + W + \frac{1}{2} m v^2 + mgz + m h \qquad (1)$$

where $m = m_2 - m_1$ (see nomenclature for definition of terms). The thermal energy in an air-rock system at States 1 and 2 (two terms on the left-hand side of equation (1)) can also be expanded as a summation of the thermal energy in the gas phase and the thermal energy in rock matrix as

$$\begin{aligned} E_1 &= m_1 C_V T_1 + m_R C_R T_1 \\ E_2 &= m_2 C_V T_2 + m_R C_R T_2 \end{aligned} \qquad (2)$$

where m_1 is the mass of air present at State 1, and m_2 is the mass of air present at State 2, and the subscript R refers to the rock (solid grains of matrix) which would be zero for cavern CAES. If heat flow (Q), work done by the system (W), kinetic energy, and potential energy are negligible, as suggested by Eq. 1 the energy change in the reservoir associated with air injection comes from the specific enthalpy (h) that is injected with the air. From the definition of the real gas law with compressibility factor Z, we have

$$\begin{aligned} m_1 T_1 &= P_1 V \tfrac{M}{ZR} \\ m_2 T_2 &= P_2 V \tfrac{M}{ZR} \end{aligned} \qquad (3)$$

Substituting the real gas law Eqs. 3 into Eq. 2, we obtain

$$E_2 - E_1 = C_V \tfrac{M}{ZR} V \left(P_2 - P_1\right) + m_R C_R \left(T_2 - T_1\right) \qquad (4)$$

where V is the volume occupied by the air. If we consider PM-CAES to occur in a reservoir of total bulk volume V_{res} with residual liquid saturation (S_{lr}) present, we can write the change in energy due to injection of a mass of air as

$$E_2 - E_1 = C_V \frac{M}{ZR} V_{res} \phi (1 - S_{lr})(P_2 - P_1) + V_{res} (1 - \phi) \rho_R C_R (T_2 - T_1) + V_{res} \phi (S_{lr}) \rho_l C_l (T_2 - T_1) \quad (5).$$

This is the essence of CAES: the enthalpy carried by the injected air is manifested as an increase in air pressure, and an increase in liquid and rock temperature. Even if the system is isothermal (i.e., $T_1 = T_2$), there is still energy storage occurring because of mass change in the system (i.e., $m_1 \neq m_2$), resulting in a pressure change. In most cases, such energy change in the reservoir is equal to the enthalpy associated with the injected (or produced) air (i.e., the terms for heat, work, kinetic, and potential energy in Eq. (1) are small). Although appealing in its simplicity, Eq. 5 does not tell the whole story about energy storage in a PM-CAES reservoir, which as we will show below is dominated by variable pressure (pressure gradients) rather than the single pressure values which can be easily evaluated at States 1 and 2 in a cavern.

There also exist concepts for constant-pressure CAES using water-column pressure compensation, e.g., for CAES in hard-rock mines (Succar and Williams 2008). In this case, with constant pressure the energy storage occurs either because of the change in volume or temperature of the reservoir. Thus, we can write the real gas law as

$$\begin{aligned} m_1 T_1 &= P V_1 \frac{M}{ZR} \\ m_2 T_2 &= P V_2 \frac{M}{ZR} \end{aligned} \quad (6)$$

And obtain the following analog to Eq. 5 for pressure-compensated cavern systems:

$$E_2 - E_1 = C_P \frac{M}{ZR} P (V_2 - V_1) \quad (7).$$

There are some efficiencies that are added in energy recovery using a constant-pressure stream of air, but there are also significant complexities added in the implementation of a water-column to compensate pressure, not the least of which is the possible exsolution of dissolved gas from water in the column as it undergoes pressure changes during cycling, the so-called champagne effect (e.g., Giramonti et al. 1978).

For isothermal cavern or PM-CAES, we can also write the stored energy in terms of the air flow rate □ as

$$E_2 - E_1 = \Delta E = \dot{m} h \Delta t \quad (8).$$

The air flow rate in and out is a convenient way to quantify the amount of energy being stored and recovered, but it does not reveal anything about processes in the reservoir.

For CAES in theory, any fluid could be used to cause a pressurization in a closed container. But for efficient energy recovery, a compressible fluid such as air is convenient because it can be expanded through a turbine. A fluid with oxygen in it is also convenient because it can be used to burn natural gas during the expansion process to avoid the extreme cooling that otherwise occurs during expansion. This tendency for extreme cooling explains why it is advantageous to add heat during air production, e.g., by recuperating heat from the effluent of the gas turbine to the produced gas as done at the McIntosh plant (Succar and Williams 2008), and why adiabatic CAES, whereby heat of compression on the storage cycle is stored for later recovery on the production cycle, is so attractive (e.g., Grazzini and Milazzo 2008).

Full Model Equations

In general, to change the pressure (or volume) in any type of fluid-pressure energy storage system, a fluid (e.g., air) must be injected and pressurized. To recover the stored energy, fluid must be produced and used to do useful work. This involves the use of a wellbore, which was not explicitly included in the system definition above. When a wellbore is included, kinetic energy, gravitational potential energy, and heat losses cannot be neglected. The complete set of mass and energy conservation equations that we solve in the simulations presented here includes mass and energy fluxes for the wellbore and the reservoir as presented in Table 1. Note in Table 1 that slightly different equations apply to the wellbore relative to those in the reservoir, e.g., kinetic energy and gravitational potential energy are important in the wellbore and negligible in the reservoir. Similarly, Darcy velocity is used in the reservoir while a velocity appropriate for pipe flow is used in the wellbore.

Methods

We have developed T2Well, a numerical simulator for solving the equations of non-isothermal, multiphase, and multi-component flows in an integrated wellbore-reservoir system (e.g., Table 1), for a variety of applications (e.g., Pan et al. 2011a, b; Oldenburg et al. 2011), including PM-CAES. T2Well extends the existing numerical reservoir simulator TOUGH2 to calculate the flow in both the wellbore and the porous medium reservoir simultaneously and efficiently by introducing a special wellbore sub-domain into the numerical grid. TOUGH2 uses a mass-conserving integral finite difference method with implicit time stepping to solve the multicomponent Darcy flow equations in the porous medium, and a residual based convergence criterion with Newton-Raphson iteration to handle non-linearity (Pruess et al., 1999). For grid blocks in the wellbore sub-domain, we solve the 1D momentum equation of the mixture (which may be two-phase) as described by the drift-flux model (DFM). The velocity of the mixture is obtained by solving the momentum equation numerically while the individual phase velocities are calculated from the mixture velocity and other fluid parameters as defined by the DFM. A mixed implicit-explicit scheme is applied to facilitate the solution of the momentum equation within the Newton-Raphson iteration framework of TOUGH2. Specifically, the pressure gradient, the gravity component, and the time derivative of momentum are treated fully implicitly while the spatial gradient of momentum is treated explicitly. The friction term is calculated with a mixed implicit-explicit scheme (Pan et al. 2011a).

This wellbore-domain approach is coupled seamlessly with the standard TOUGH2 porous media approach to simulate coupled wellbore-reservoir flow problems, e.g., wellbore leakage and injection relevant to geologic carbon sequestration (Pan et al. 2011b) and oil reservoir blowout (Oldenburg et al. 2011). The rigor of the flow modeling in T2Well is matched by the accuracy of the equation of state (EOS) modules used for the fluid compositions and phase relations. In this study, we make use of TOUGH2/EOS3 (Pruess et al., 1999) which models two fluid phases (aqueous and gaseous), and two chemical components (H_2O and air, a pseudocomponent).

Prototypical PM-CAES Example

Introduction

In order to address the four general questions posed above about PM-CAES, we present simulations of the performance of a hypothetical idealized PM-CAES system operated with the same schedule and injection-production rates as the Huntorf cavern CAES system. The results are used to show how PM-CAES systems work generally rather than to consider the sensitivity of results to parameter variations. The work presented here also demonstrates the simulation capability itself which can of course be applied to more specific systems or to further studies of parameter sensitivity or PM-CAES system design.

Description

The prototypical PM-CAES system considered here consists of an axisymmetric domain composed of a single wellbore partially penetrating a gently domed isotropic reservoir with hydrostatic conditions in the far-field water leg as shown in Figure 1. Properties of the reservoir and wellbore are given in Table 2. Typical properties of a high-permeability (1 Darcy) sandstone reservoir and large-diameter well (~0.5 m) are chosen in order to accommodate large flow rates. The well is discretized as a one-dimensional domain with 10 m vertical grid spacing gradually reducing to 1 m vertical spacing as the well approaches the reservoir. The reservoir is discretized into a radially symmetric mesh with vertical resolution of 1 m and lateral resolution varying from 0.1 m near the wellbore to 100 m in the far-field for a total of 2827 grid blocks.

The top and bottom of the dome structure of the reservoir are closed to heat and mass transfer, and open with constant hydrostatic P and geothermal-gradient T on the down-dip water leg. The well is closed to mass flow all along its length except where it is perforated for 30 m in the reservoir. Heat exchange between the wellbore and the formation above the reservoir is modeled using Ramey's semi-analytical solution for conductive heat flow (Ramey 1962).

The initial condition of the reservoir consists of a gas cap above a saturated water leg at gravity-capillary equilibrium as shown in Figure 2a. Although we do not consider methane (CH_4) in the model, this initial condition mimics one possible state of a natural gas reservoir. We chose this initial condition to avoid complications of simulating the transient development of the initial bubble that would occur in the start-up of an aquifer CAES project, and to avoid the problem of separating out fundamental long-term pseudo-steady PM-CAES behavior from the behavior associated with this transient bubble-formation.

Cyclic CAES injection and production flow rates were set equal to one-half of Huntorf's air injection and production which occurs in two caverns with total volume of 3.1×10^5 m^3. Energy storage is modeled by specification of a mass and enthalpy source term for the 12-hour storage period at the top of the well as given in Table 3. The CAES operation is simulated by injecting a mixture of pseudocomponent air plus water vapor with a given enthalpy corresponding to humid air at 50 °C. Energy recovery for three hours each day is specified by the production of mass at the top of the well at one-half the Huntorf production rate. The 4.5-hour shut-in periods are specified by zeroing out the injection and production rate at the wellhead and simulating wellbore and reservoir relaxation. We do not model any of the surface infrastructure of the system (e.g., piping, compressors, turbines, etc.).

Results

We present in Figure 2b-d some snapshots of the pressure and liquid saturation fields at various times in the energy storage and production cycle to demonstrate two-phase fluid flow and pressurization in the reservoir. In order to show how these 2D radial simulation results translate into energy storage by PM-CAES, we show in Figure 3 the continuous cyclic variation of pressure at the top of the well (wellhead), bottom of the well (down hole), and four different places in the reservoir progressively farther from the well at the mid-point in thickness of the reservoir. As shown, the reservoir pressure increases during the initial fill period and then oscillates during each production, shut-in, recharge, and shut-in cycle with most of the variation occurring in and near to the well. The restriction of variation in pressure to the well and to near-well regions is caused by the presence of porous medium in the reservoir which limits air flow and

therefore the extent to which injection-related pressure propagates over time. A similar plot of pressure evolution at various locations within a cavern, e.g., at Huntorf, would show nearly uniform pressure throughout the cavern at any given height because the open cavern allows very rapid pressure propagation. We note also that production in our example PM-CAES system is at constant rate to ensure it is comparable to the Huntorf system. The resulting pressure profiles for the wellhead vary by about 1.4 MPa over the production period, which suggests a similar production rate would arise from specification of constant wellhead pressure at about 1.4 MPa below the shut-in pressure.

We show in Figure 4 the evolution of temperature in the reservoir during the initial fill and throughout 100 cycles. As with pressure evolution, the temperature variation with time is limited to regions in and very near to the well. In porous media, the propagation of thermal fronts by advection (aka convection) is retarded by heat absorption by the solid grains of the matrix (e.g., Bodvarsson 1972; Oldenburg and Pruess 1999). In PM-CAES, heat can be exchanged back and forth between the air, the solid grains, and any residual phases (e.g., an aqueous phase such as in the present example). This effect and its reversibility tend to limit the changes in temperature that occur during repeated cycling of air in the reservoir. The decline in temperature at the wellhead during the shut in period is due to heat transfer away from the well (cooling) into the surrounding (shallow) formation which is at a temperature controlled by the imposed geothermal gradient. The short-duration decline in temperature at the wellhead upon start of production after shut in is due to the instantaneous imposition of mass extraction at the top of the well and the associated cooling. During the transition from shut in to recharge, the excursion in temperature at the wellhead does not appear because both the injection of air at 50 °C and the related compression of air in the well lead to positive temperature change. Similarly, there is no temperature excursion at the wellhead during the transition from recharge to shut-in because air at the wellhead tends to decompress and cool by conduction into the shallow formation leading to decreasing temperature by both effects. The long-term heating trend in the wellhead temperature occurs because over time the formation around the wellbore

heats up relative to the initial geothermal gradient condition as heat is lost from warm (T = 50 °C) injected air; thus less heat is lost over time.

As the above results suggest, the reservoir performance is coupled to the wellbore, and our simulation rigorously models this coupling. We show in Figure 5 the evolution of pressure and temperature throughout the entire length of the wellbore during the 100 daily cycles of PM-CAES, and over two cycles (inset) to show the details. Figures 5a-b nicely show the recharge, shut-in, and production *P*-*T* behavior in the well as controlled by production and injection specification at the wellhead, and as controlled by the reservoir.

Questions about PM-CAES

With this rigorous simulation of an idealized PM-CAES reservoir in hand, we are now in a position to address the four fundamental questions about PM-CAES.

Question 1: Can pore space provide large-scale energy storage?

Although the answer to this question will seem obvious to many readers, we include it here along with discussion because we have observed that a PM-CAES reservoir stores energy differently (spatially) from how a cavern stores energy. Before getting into the discussion, we present the kind of summary result that most readers will have expected. Shown in Figure 6 is the evolution of energy flow rate (in W) at the six different locations in the well and reservoir. As shown, energy that goes into the system during recharge is held by the system during shut in, and is recovered during the production of air. Note that the rate of energy extraction (68 MW) is not equal to one-half of Huntorf (145 MW) because Huntorf's nominal turbine output includes the energy produced by the heating rate (added natural gas in the gas turbine). The rate calculated in our simulation looks reasonable if we consider the rule of thumb that CAES plants burn about 25-50% of the natural gas normally required for a given generation rate of the turbine (68 MW = 0.47 × 145 MW) and we do not account for inefficiency in energy recovery above the wellhead.

But summary results such as those in Figure 6 do not elucidate the way that energy is stored in the reservoir. Recall that CAES occurs primarily as a $V\mathrm{d}P$ term (e.g., Eq. 4). In caverns, the dP occurs throughout the entire cavern because there is no resistance to air flow in an open cavern. In contrast, in PM-CAES, there is large resistance to air flow provided by the porous medium and this results in pervasive pressure gradients established by the injection of air. Pressure gradients remains throughout the injection period. During shut in, the gradient tends to diminish but it does not disappear entirely in the reservoir during shut in even in the high-permeability idealized PM-CAES system studied here. During the production of air, the pressure gradient reverses and air flows toward and up the well. This can be seen in Figures 2b and c by the persistence of pressure variation in the gas cap. Therefore, energy storage is spatially variable in the reservoir depending on dP, which depends on the distance of the air-filled pores from the well. This is very different from the cavern case where energy is stored uniformly throughout the cavern at nearly constant pressure. In summary, our simulations show that large-scale energy storage can be carried out using the pore space of geologic reservoirs, with energy storage occurring variably throughout the reservoir depending on distance from the well.

In contrast to cavern CAES, pressure gradients in the reservoir will be the norm during storage and recovery cycles in PM-CAES. Of course very long shut-in periods could allow pressure equilibration in certain high-permeability compartmentalized reservoirs, but upon production of air, energy recovery will occur in a spatially varying manner as low pressures will occur first near the well and only later propagate outward to the boundaries of the compartment.

Question 2: What is the efficiency of the coupled wellbore-reservoir system for storing energy?

The efficiency of CAES is one of the primary issues for feasibility. Efficiency can be evaluated in many different ways as summarized by Succar and Williams (2008). As earth scientists, we ignore the various arcane choices about efficiency definitions involving heating rate (added natural gas) and compressor and turbine efficiency and restrict our consideration to the subsurface part of the PM-CAES system (wellbore plus reservoir) where efficiency can be simply defined as the ratio of energy (or mass) out divided by

energy (or mass) in. Shown in Figure 7 are the ratios of produced mass and energy to injected mass and energy, respectively, per cycle. Ratios are presented for the top of the reservoir at the wellhead to distinguish reservoir losses from wellbore losses. As shown, mass and energy are very efficiently stored in the reservoir. Mass losses are about 3.5% which is the same make-up injection as used at the Huntorf plant. Corresponding energy losses can be found at the top of the reservoir because less mass is produced than injected on each cycle. The energy efficiency is slightly lower at the wellhead due to heat losses along the wellbore.

Question 3: Does pressure diffusivity affect storage efficiency?

Pressure diffusivity is an analogy to thermal and molecular diffusivity that indicates the rate at which pressure signals caused by fluid flow will propagate in porous media. Pressure diffusivity has dimensions of $L^2\ T^{-1}$ and is defined as the ratio of transmissivity (T) to storativity (S) for a formation of thickness b and compressibility α by

$$D = \frac{T}{S} = \frac{\frac{k\rho g}{\mu} b}{\rho g b(\alpha + \phi\beta_f)} = \frac{\frac{k}{\mu}}{\alpha + \phi\beta_f} \qquad (9)$$

where k, ϕ, ρ, μ, and β_f are the fluid permeability, porosity, density, viscosity, and compressibility, respectively (Freeze and Cherry 1978). The pressure diffusivity of water (aqueous phase) is always larger (approximately four to 10 times larger at 50 bar) than it is for air. The concern for PM-CAES is either that (1) the pressure diffusivity would be very small and thereby slow down the recovery of air from the reservoir and limit the rate at which air could be injected, or (2) that pressure diffusivity would be very large and injection would not be able to create a lasting pressurization (dP) in the case of an open reservoir.

In our prototypical PM-CAES system, where pressure diffusivity varies across the system due to variable saturation and pressure, we did not observe any detrimental behavior due to small pressure diffusivity.

Instead, the wellbore contact with the reservoir was the limiting factor for flow rate and we had to make the wellbore have a fairly large diameter (0.5335 m, same as that used at Huntorf) in order to contact a sufficient area of the reservoir to achieve the Huntorf injection and production rates. As for pressure gradients produced in the reservoir, the system showed itself to be highly reversible over the daily cycle simulated. As discussed in the comments to Question 1, energy storage density will always be spatially variable in the formation because of pressure gradients in the reservoir. Our simulations show that these gradients reverse themselves, and the reservoir and wellbore parts of PM-CAES are very efficient for energy storage (e.g., Figure 7).

As for large pressure diffusivity, this was not a problem in our prototypical system because we had closed boundaries on the top and bottom of the dome structure, a gas-water contact on the down-dip water leg, and a pore volume commensurate with the chosen injection rate, all of which created an effective compartment. But clearly in general, large pressure diffusivity could be an issue in a PM-CAES system that could cause the inability to generate and sustain a desired dP for the available injection rate. In short, PM-CAES systems must be in appropriately sized reservoirs with a pore volume bounded by hydrologic or cap rock seals that provide a barrier against pressure diffusion over the time scales needed to store energy. Such appropriate size of a reservoir is related to the given operation scale in terms of injection/production rates. In many cases, multiple wells would be needed to utilize a large reservoir with large storage capacity.

Question 4: Is energy lost due to air moving water around in the reservoir?

One of the concerns of PM-CAES is that injected air will do work on the water held in the pore space and thereby lose energy as it moves water around in the reservoir. The initial condition we use is a gravity-capillary equilibrium, which means that water (aqueous phase) is held stationary in the pores of the gas cap as controlled by gravity and capillary pressure with no-flow of gas (e.g., air) in the system. Upon injection or production of air during PM-CAES, there is the possibility that flowing air would disrupt this equilibrium, and effectively move water around in the reservoir, and thereby lose energy. Our simulation

results show that injected air does not move water around except by vaporization (dry out) in the vicinity of the well during initial injection. As shown in Figure 8, the gas-phase saturation does not change during the 100 daily cycles simulated, even very close to the well. This result is in agreement with theoretical analyses which show that the time scale for water flow is much longer than for air flow (Katz and Lady 1976; Succar and Williams 2008). Changes in gas saturation do occur at the bottom of the well (down hole), but this reduction in gas-phase saturation actually reflects the occurrence of aqueous phase that condenses in the well. Gas saturation could also change in the system due to evaporation as air dries the formation. However, we injected moist air in our simulation to avoid this effect in order to focus on flow-related water mobilization.

Conclusions

We have developed and demonstrated a rigorous coupled wellbore-reservoir simulation capability to address four fundamental questions about the performance of PM-CAES. Applying this new capability to a single prototypical PM-CAES system, we find first that PM-CAES systems store energy in a spatially variable manner according to the variable pressure in the reservoir. We find second that the wellbore-reservoir part of the PM-CAES system is very efficient at storing energy, at least for the idealized system we simulated. As for pressure diffusivity, formations with either too small or too large a value of pressure diffusivity will not be favorable for PM-CAES. Rather, systems need to have appropriate permeability, sealing characteristics, and size to be good PM-CAES systems. Finally, we confirmed the expectation that injected air does not appreciably move water around once a gravity-capillary equilibrium has been established during cycling operation. The significance of this result is that injected air will not lose energy by doing work on the residual water in the formation.

While this work has addressed four fundamental questions, there are many other issues that we believe need to be addressed more thoroughly than in the past regarding geochemical and biogeochemical impacts of air injection, geomechanical aspects of repeated cycling of pressure, treatment of high

velocities near the well, and synergies that can potentially occur between PM-CAES, enhanced hydrocarbon recovery, and geologic carbon sequestration. Our simulation capabilities and extensions can be used for future investigations of these and other aspects of PM-CAES.

Acknowledgments

We thank Paul Denholm (NREL), Samir Succar (NRDC), Joe Chan (PGE), Vasilis Fthenakis (Columbia University), and Steve Webb (Canyon Ridge Consulting) for helpful discussions regarding CAES. We also thank Christine Doughty and Matthew T. Reagan (LBNL) for helpful discussion and internal review of an earlier draft. This work was supported in part by the Office of Science, U.S. Department of Energy, and by the Assistant Secretary for Fossil Energy (DOE), Office of Coal and Power Systems, through the National Energy Technology Laboratory (NETL), and by Lawrence Berkeley National Laboratory under Department of Energy Contract No. DE-AC02-05CH11231.

References

Allen, K., 1985. CAES: The underground portion, *IEEE Power Engineering Review*, April 1985, p. 35.

Allen, R.D., T.J. Doherty, and L.D. Kannberg, 1985. Summary of selected compressed air energy storage studes, Pacific Northwest Laboratory Report *PNL-5091/UC-94e*.

Bodvarsson, G., 1972. Thermal problems in the siting of reinjection wells, *Geothermics*, *2*, 63-66.

Braester, C., and J. Bear, 1984. Some hydrodynamic aspects of compressed-air energy storage in aquifers, *J. of Hydrology*, *73*, 201-225.

Cavallo, A., 2007. Controllable and affordable utility-scale electricity from intermittent wind resources and compressed air energy storage (CAES), *Energy*, *32*, 120-127.

Corey, A.T., 1954. The interrelation between gas and oil relative permeabilities, *Producers Monthly*, 38-41, November 1954.

Crotogino, F., K.-U. Mohmeyer, and R. Scharf, 2001. Huntorf CAES: More than 20 years of successful operation, Spring 2001 Meeting of the Solution Mining Research Institute, Orlando, FL, 15-18 April 2001.

Denholm, P; and Kulcinski, GL, 2004. Life cycle energy requirements and greenhouse gas emissions from large scale energy storage systems, *Energy Conv. Mgt.*, *45*, 2153-2172.

Denholm, P.; R. Sioshansi, 2009. The value of compressed air energy storage with wind in transmission-constrained electric power systems, *Energy Policy*, *37*, 3149-3158.

EPRI (Electrial Power Research Institute), 2010. *Electric Energy Storage Technology Options, A Primer on Applications, Costs & Benefits*, EPRI, Palo Alto, CA.

Freeze, R.A., and J.A. Cherry, 1979. *Groundwater*, Prentice Hall, Englewood Cliffs, NJ, 604 pp.

Giramonti, A.J., R.D. Lessard, W.A. Blecher, and E.B. Smith, 1978. Conceptual design of compressed air energy storage electric power systems, *Applied Energy*, *4*(4), 231–249.

Grazzini, G., and A. Milazzo, 2008. Thermodynamic analysis of CAES/TES systems for renewable energy plants, *Renewable Energy*, *33*, 1998-2006.

Katz, D.L., and E.R. Lady, 1976. *Compressed air storage for electric power generation*, Ulrich's Books Inc., 244 pp.

Kim, HM; Rutqvist, J; Ryu, DW; Choi, BH; Sunwoo, C; Song, WK, 2012. Exploring the concept of compressed air energy storage (CAES) in lined rock caverns at shallow depth: A modeling study of air tightness and energy balance, *Applied Energy*, *92*, 653-667.

Kushnir, R., A. Ullmann, and A. Dayan, 2010. Compressed air flow within aquifer reservoirs of CAES plants, *Trans. Porous Media*, *81*, 219-240.

Kushnir, R., A. Dayan, and A. Ullmann, 2012. Temperature and pressure variations within compressed air energy storage caverns, *Int. J. Heat Mass Trans.*, *55*, 5616-5630.

Meiri, D., and G.M. Karadi, 1982. Simulation of air storage aquifer by finite element model, *Int. J. for Num. and Analyt. Meths. in Geomechs.*, *6*, 339-351.

Oldenburg, C.M., and K. Pruess, 1999. Plume separation by transient thermohaline convection in porous media, *Geophys. Res. Lett., 26*(19), 2997–3000.

Oldenburg, C.M., B.M. Freifeld, K. Pruess, L. Pan, S.A. Finsterle, and G.J. Moridis, 2011. Numerical simulations of the Macondo well blowout reveal strong control of oil flow by reservoir permeability and exsolution of gas, *Proc. National Acad. Sci.*, *Early Edition*, July 5, 2011.

Pan, L., C. M. Oldenburg, Y. Wu and K. Pruess, 2011a. T2Well/ECO2N Version 1.0: Multiphase and Non-Isothermal Model for Coupled Wellbore-Reservoir Flow of Carbon Dioxide and Variable Salinity Water, Report *LBNL-4291E*, Lawrence Berkeley National Laboratory, Berkeley, Calif..

Pan, L., C.M. Oldenburg, K. Pruess, and Y.S. Wu, 2011b. Transient CO_2 leakage and injection in wellbore-reservoir systems for geologic carbon sequestration, *Greenhouse Gases: Science and Technology*, *1*(4), 335–350.

Pruess, K., 2004. The TOUGH Codes—A family of simulation tools for multiphase flow and transport processes in permeable media, *Vadose Zone Journal*, *3*(3), 738-746.

Pruess, K., C.M. Oldenburg and G.J. Moridis, 1999. TOUGH2 User's Guide Version 2. E. O. Lawrence Berkeley National Laboratory Report *LBNL-43134*.

Ramey, H.J. Jr., 1962. Wellbore heat transmission. *J. Pet. Tech.*, *225*, 427–435.

Rutqvist, J; Kim, HM; Ryu, DW; Synn, JH; Song, WK, 2012. Modeling of coupled thermodynamic and geomechanical performance of underground compressed air energy storage in lined rock caverns, *Int. J. Rock Mech. and Mining Sci.*, *52*, 71-81.

Schainker, R.B.; M. Nakhamkin, 1985. Compressed Air Energy Storage (CAES) – Overview, performance, and cost data for 25 MW to 220 MW plants, *IEEE Transactions on Power Apparatus and Systems*, *PAS-104* (4), 791-795.

Succar, S., and R.H. Williams, 2008. *Compressed air energy storage: Theory, resources, and applications for wind power*, Energy Analysis Group, Princeton University, 81 pp.

Raju, M., and S.K. Khaitan, 2012. Modeling and simulation of compressed air storage in caverns: A case study of the Huntorf plant, *Applied Energy*, *89*, 474-481.

Schulte, R.H., N. Critelli Jr., K. Holst, and G. Huff, 2012. Lessons from Iowa: Development of a 270 MW compressed air energy storage project in Midwest Independent System Operator, Sandia Report *SAND2012-0388*.

Westervelt, A., 2010, PG&E Approved for $50 Million Compressed Air Energy Storage Project, *InsideClimate News*, http://insideclimatenews.org/news/20100131/pge-approved-50-million-compressed-air-energy-storage-project (accessed July 25, 2012).

Nomenclature

A	wellbore cross-sectional area	m^2
b	formation thickness	m
C_0	shape factor	-
C_R	heat capacity of the rock	J kg^{-1} K^{-1}
C_P	heat capacity at constant pressure	J kg^{-1} K^{-1}
C_V	heat capacity at constant volume	J kg^{-1} K^{-1}
D	pressure diffusivity	m^2 s^{-1}
g	acceleration of gravity vector	m s^{-2}
E	Energy	J
F	Darcy flux vector	kg m^2 s^{-1}
H	enthalpy	J
h	specific enthalpy	J kg^{-1}
k	permeability	m^2
k_r	relative permeability	-
m	mass	kg
m_{vG}	van Genuchten (1980) parameter	-
□	mass flow rate of air	kg s^{-1}
M	mass accumulation term, molecular weight	kg m^{-3}, kg mol^{-1}

n	empirical parameter in van Genuchten model	
n	outward unit normal vector	-
NK	number of components	-
NPH	number of phases	-
q"	heat loss/gain transverse to wellbore	J s^{-1} m^{-2}
P	total pressure	Pa
P_{cmax}	maximum capillary pressure	Pa
P_{c0}	aqueous-gas capillary pressure strength	Pa
Q	heat	J
q_v	volumetric source term	kg m^{-3} s^{-1}
R	radial coordinate, gas constant	m, J kg^{-1} mol^{-1}
S	saturation, storativity	-, m^{-1}
t	time	s
T	temperature, transmissivity	^{o}C, m s^{-1}
u	*Darcy* velocity of phase β	m s^{-1}
uG, uL	*phase velocity of gas and liquid in the well*	m s^{-1}
U	internal energy	J kg^{-1}
v	*velocity*	m s^{-1}
V	volume	m^3

W	work	J
X	mass fraction w/phase subscript and component superscript	
z	Z-coordinate (positive upward)	m
Z	compressibility factor	-

Greek symbols

α	fluid compressibility	Pa^{-1}
β	phase index	
β_f	formation compressibility	Pa^{-1}
Γ	surface area	m^2
θ	angle between wellbore and the vertical	°
κ	mass components (superscript)	-
λ	thermal conductivity of fluid-rock composite	$J\ m^{-1}\ s^{-1}\ K^{-1}$
μ	dynamic viscosity	$kg\ m^{-1}\ s^{-1}$
ρ	density	$kg\ m^{-3}$
ρ_m*	profile-adjusted average density	$kg\ m^{-3}$
τ	tortuosity	-
ϕ	porosity	-

Subscripts and superscripts

β	phase index
cap	*capillary*
d	drift
G	gas
κ	component index
l	liquid
lr	liquid residual
L	liquid
m	mixture
NK1	energy component
0	reference value
r	relative
res	bulk reservoir

Tables

Table 1. Governing equations solved in T2Well for PM-CAES.

Description	Equation
Conservation of mass or energy	$\frac{d}{dt}\int_{V_n} M^\kappa dV = \int_{\Gamma_n} \mathbf{F}^\kappa \cdot \mathbf{n} d\Gamma + \int_{V_n} q_v{}^\kappa dV$
Mass accumulation	$M^\kappa = \phi \sum_{\beta=1}^{NPH} S_\beta \rho_\beta X_\beta^\kappa$
Reservoir Domain	
Phase flux (reservoir)	$\mathbf{F}^\kappa = \sum_{\beta=1}^{NPH} X_\beta^\kappa \rho_\beta \mathbf{u}_\beta$
Energy flux (reservoir)	$\mathbf{F}^\kappa = -\lambda \nabla T + \sum_{\beta=1}^{NPH} h_\beta \rho_\beta \mathbf{u}_\beta$
Energy accumulation (reservoir)	$M^\kappa = (1-\phi)\rho_\beta C_R T + \phi \sum_{\beta=1}^{NPH} \rho_\beta S_\beta U_\beta$
Wellbore Domain	
Momentum equation (wellbore)	$\frac{\partial}{\partial t}(\rho_m u_m) + \frac{1}{A}\frac{\partial}{\partial z}\left[A \sum_{\beta=1}^{NPH} \rho_\beta u_\beta^2\right] = -\frac{\partial P}{\partial z} - \frac{\Gamma f \rho_m \lvert u_m \rvert u_m}{2A} - \rho_m g \cos\theta$
Phase flux (wellbore)	$u_G = C_0 \frac{\rho_m}{\rho_m{}^*} u_m + \frac{\rho_L}{\rho_m{}^*} u_d$ $u_L = \frac{(1-S_G C_0)\rho_m}{(1-S_G)\rho_m{}^*} u_m + \frac{S_G \rho_G}{(1-S_G)\rho_m{}^*} u_d$
Energy flux (wellbore)	$\mathbf{F}^{NK1} = -\lambda \frac{\partial T}{\partial z} - \frac{1}{A}\sum_{\beta=1}^{NPH} \frac{\partial}{\partial z}\left(A \rho_\beta S_\beta \mathbf{u}_\beta \left(h_\beta + \frac{h_\beta{}^2}{2}\right)\right)$ $- \sum_{\beta=1}^{NPH} (\rho_\beta S_\beta \mathbf{u}_\beta g \cos\theta) - q''$
Energy accumulation (wellbore)	$M^{NK1} = \sum_{\beta=1}^{NPH} \rho_\beta S_\beta \left(U_\beta + \frac{1}{2} u_\beta^2\right)$

Table 2. Properties of the prototypical PM-CAES system.

Reservoir Properties	
Reservoir dome thickness	50 m
Depth of top of dome	720 m
Porosity (ϕ)	0.20
Permeability (k)	1.0×10^{-12} m^2
Density of grains in reservoir formation	2600 kg/m^3
Compressibility of reservoir formation	1×10^{-10} Pa^{-1}
Thermal conductivity of reservoir saturated reservoir formation[4]	2.51 W/(m K)
Heat capacity (C_P) of saturated reservoir	920 J/(kg K)
Capillary Pressure (P_{cap}) and Relative Permeability (k_r) *Terminology:* m = 1-1/n = power in expressions for P_{cap} and k_r S_{ar} = aqueous-phase residual saturation S_{gr}= gas-phase residual saturation P_{c0} = capillary pressure strength between aqueous and gas phases P_{cmax} = maximum possible value of P_{cap}	van Genuchten[1] P_c and k_r with Corey[2] relative permeability for gas m_{vG} = 0.20 S_{ar} = 0.25 for P_{cap}, 0.27 for k_r S_{gr} = 0.01 P_{c0} = 1189 Pa P_{cmax} = 1 x 10^5 Pa
Initial pressure of dome	Gas-static in gas cap, hydrostatic in water leg, P top of dome = 7.2×10^6 Pa
Initial temperature of dome	Variable assuming geothermal gradient of 34.7 °C/km and T = 40 °C at 720 m depth (top of dome)
Initial saturation of dome	Variable gravity-capillary equilibrium assuming gas-water contact at Z = -60 m
Well Properties	
Well length and diameter	720 m to dome top, × 0.5335 m diameter
Well screen length	30 m in top of dome

[1]van Genuchten (1980)
[2]Corey (1954)

Table 3. Operation cycle of the prototypical PM-CAES system.

Operational Parameters	
Injection rates	Air 53.992 kg/s; H_2O 0.008 kg/s; enthalpy 3.1983×10^5 J/kg
Production rate (at top of dome)	208.5 kg/s (mass production)
Initial injection period	15 days
Daily schedule	12 hr recharge 4.5 hr shut in 3 hr production 4.5 hr shut in

Figures

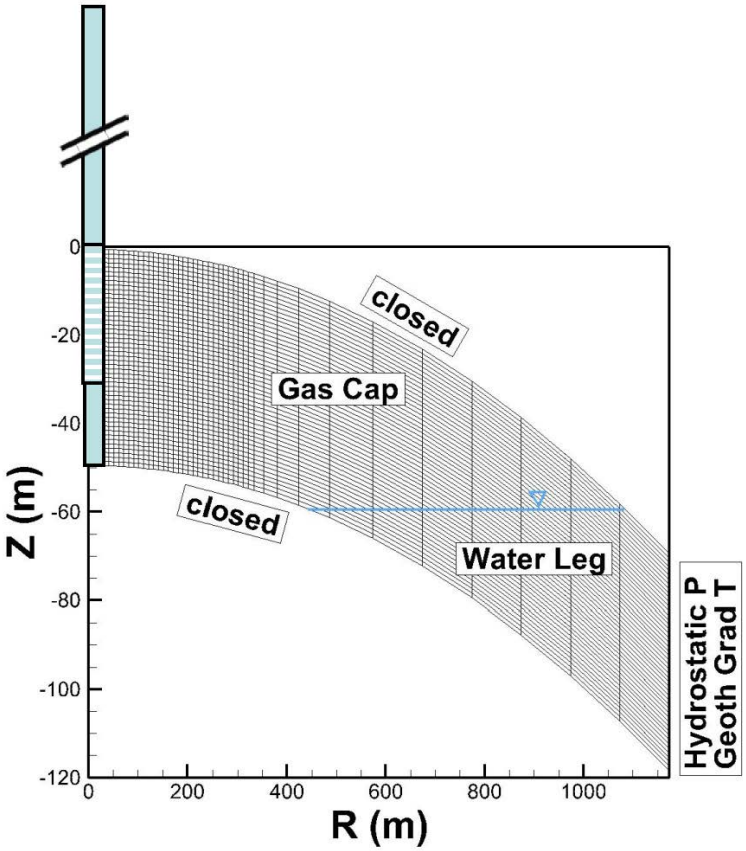

Figure 1. Domain of coupled wellbore-reservoir for prototypical CAES example (note vertical exaggeration). The well is shown (not to scale) in cyan with screened interval 0 - -30 m. The discretization in the reservoir shows the high-resolution region near the wellbore and coarser discretization for R > 400 m from the well. The top and bottom of the reservoir are closed to heat and mass flow, while the down-dip right-hand side has constant hydrostatic pressure and temperature corresponding to a geothermal gradient.

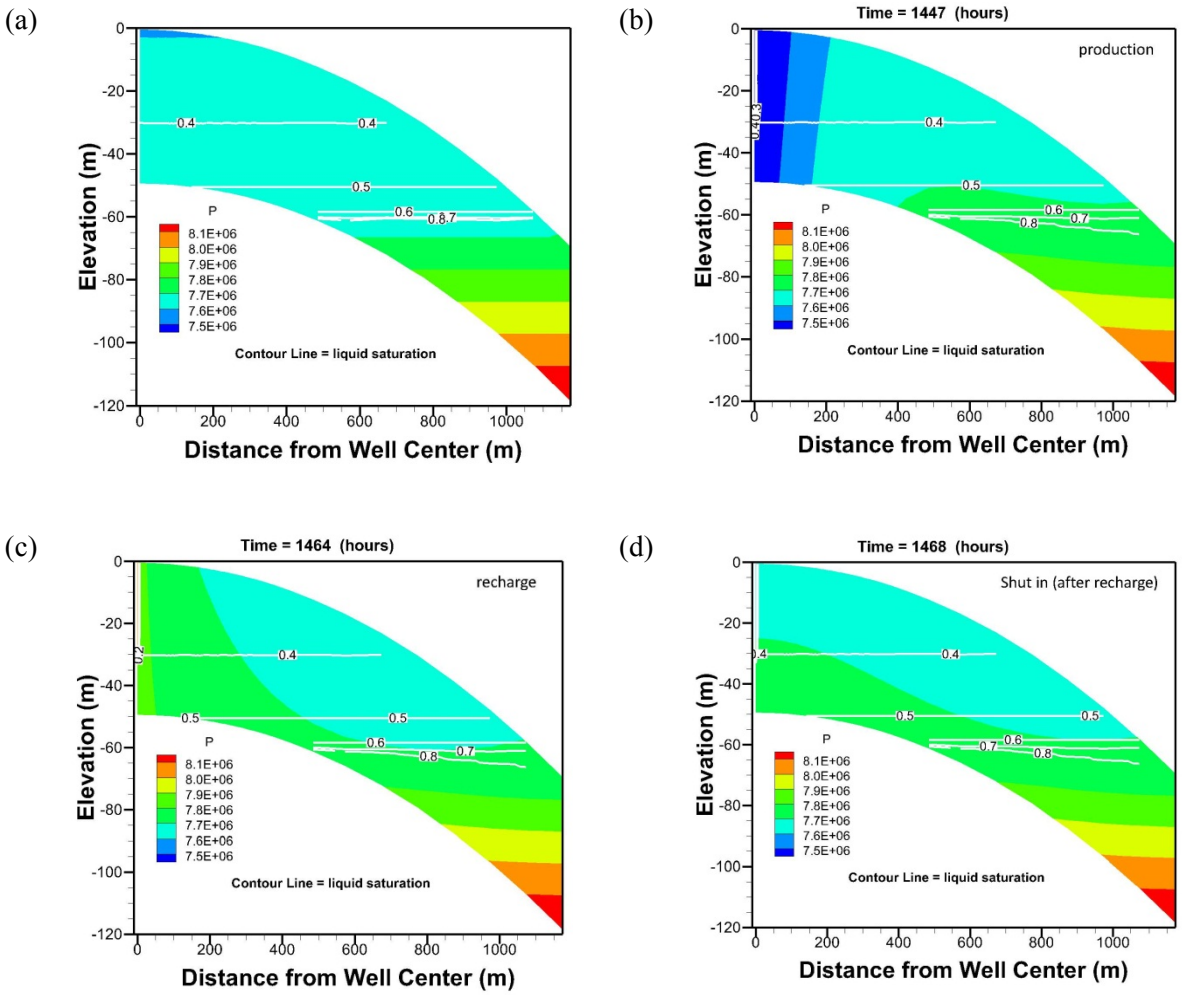

Figure 2. Snapshots of simulation results of pressure (color contours) and aqueous phase saturation (white contour lines) at four different times: (a) initial condition; (b) during air production following a recharge event; (c) during air recharge; and (d) during shut in.

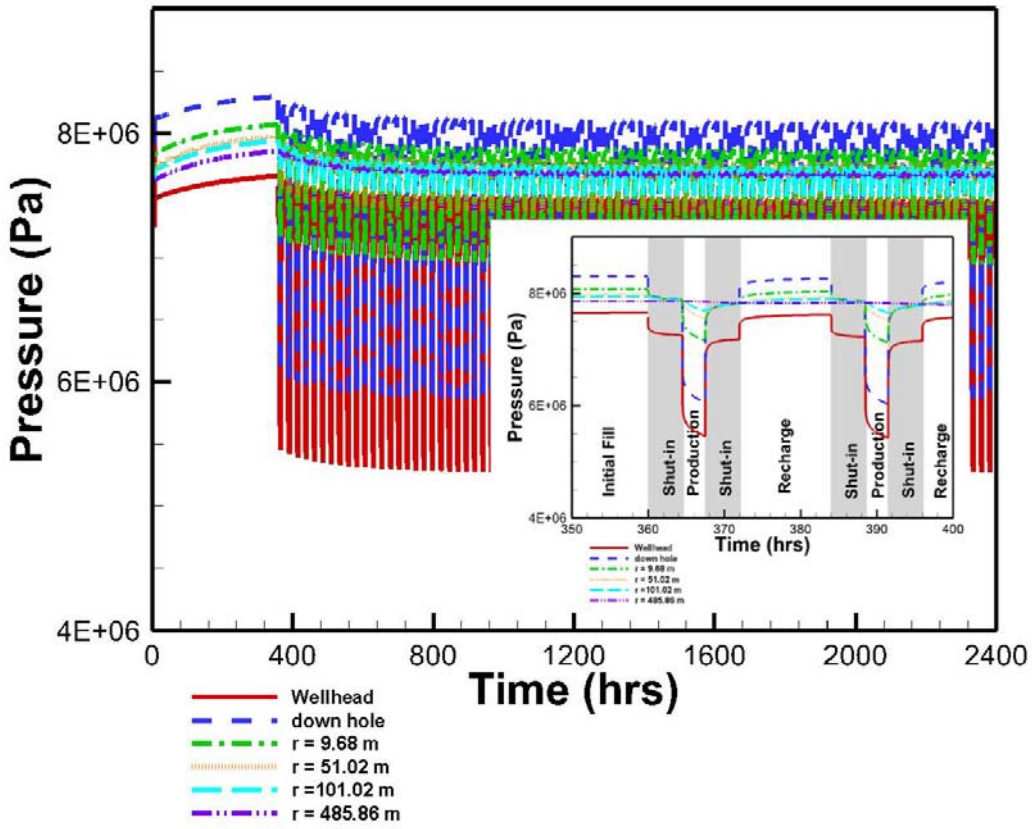

Figure 3. Evolution of pressure at six different locations in the reservoir during initial fill of air and over 100 daily cycles, and over two cycles (inset) to show detail. The results at various values of r (radius from well) are at the midpoint of thickness in the reservoir.

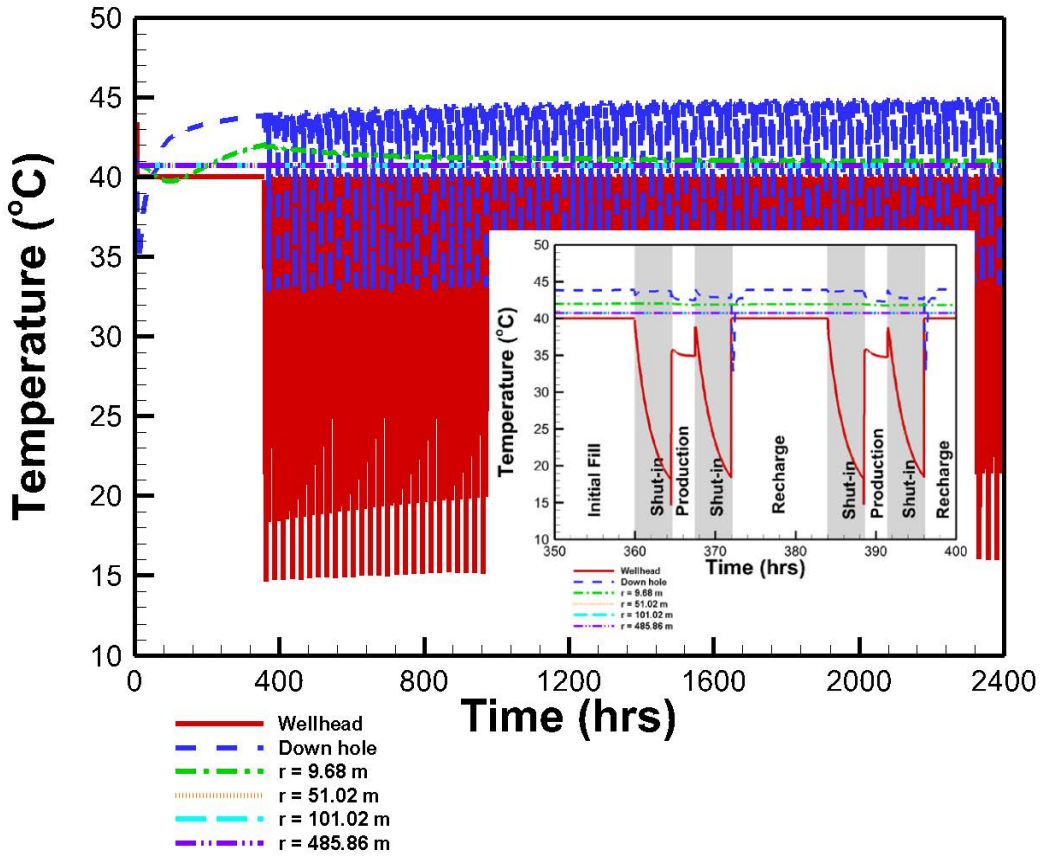

Figure 4. Evolution of temperature at six different locations in the reservoir during initial fill of air and over 100 daily cycles, and over two cycles (inset) to show detail. The results at various values of r (radius from well) are at the midpoint of thickness in the reservoir.

(a)

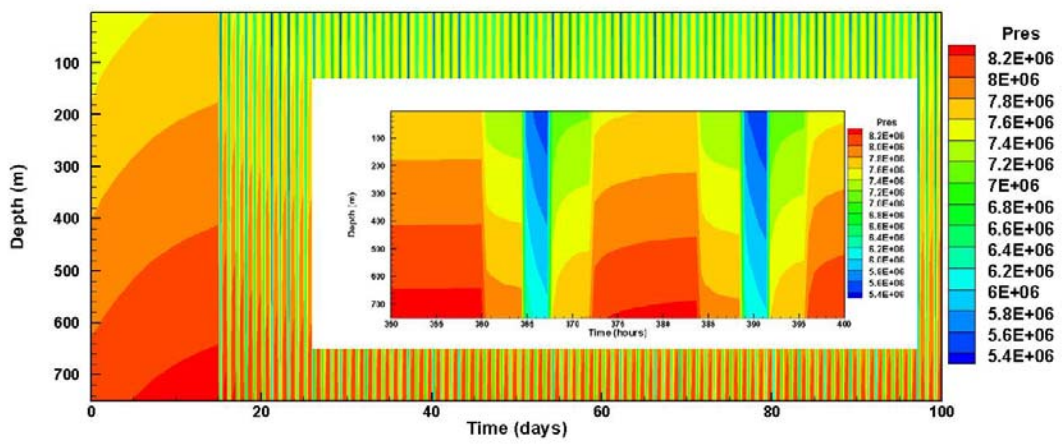

(b)

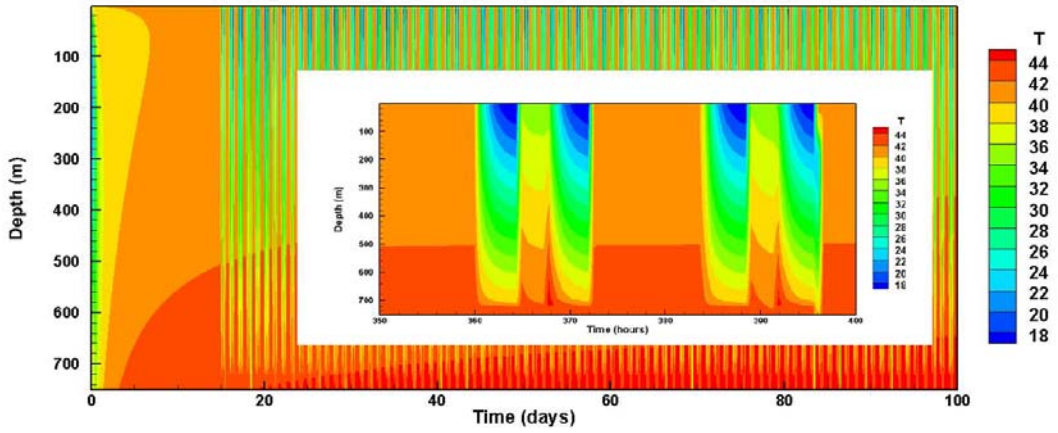

Figure 5. Simulated pressure (Pa) and temperature (°C) evolution throughout the entire length of the wellbore during 100 daily cycles of PM-CAES, along with insets showing greater detail over two cycles.

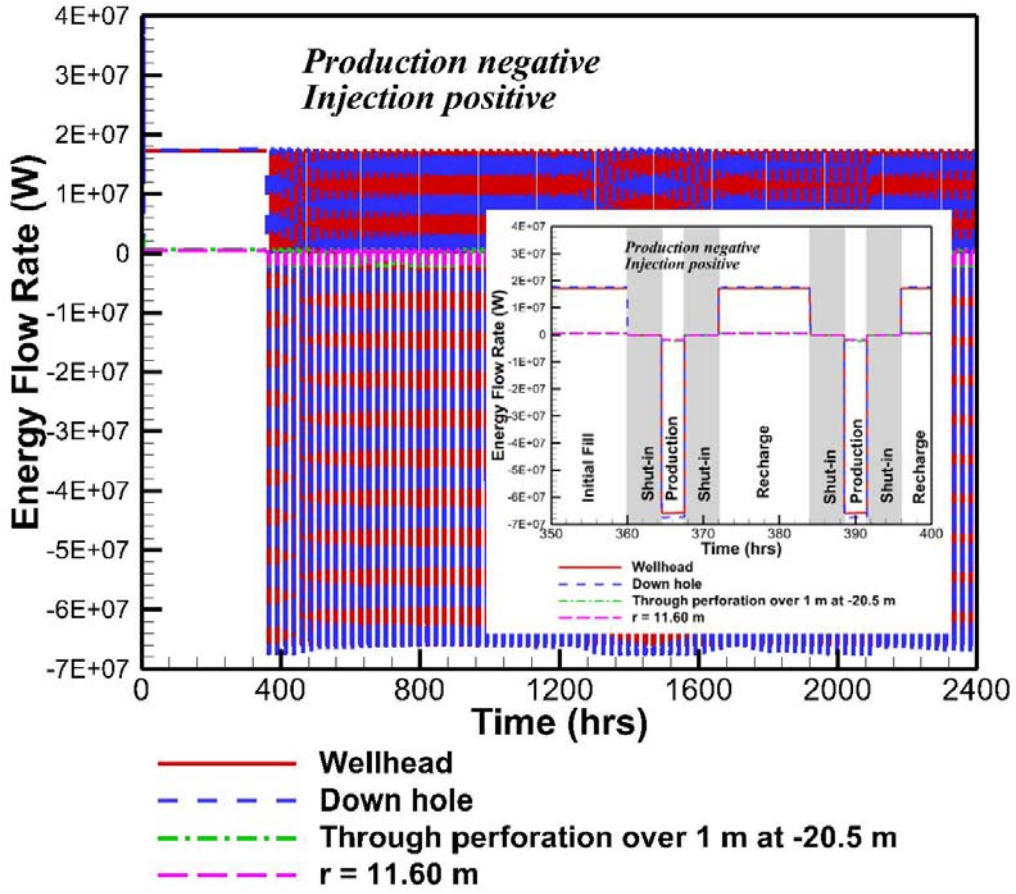

Figure 6. Energy flow at four different locations in the reservoir during initial fill of air and over 100 daily cycles, and over two cycles (inset) to show detail. The results at r (radius from well) equal to 11.6 m are at the midpoint of thickness in the reservoir. The down hole cumulative flow rate is the total energy flow gathered over the length of the perforated well.

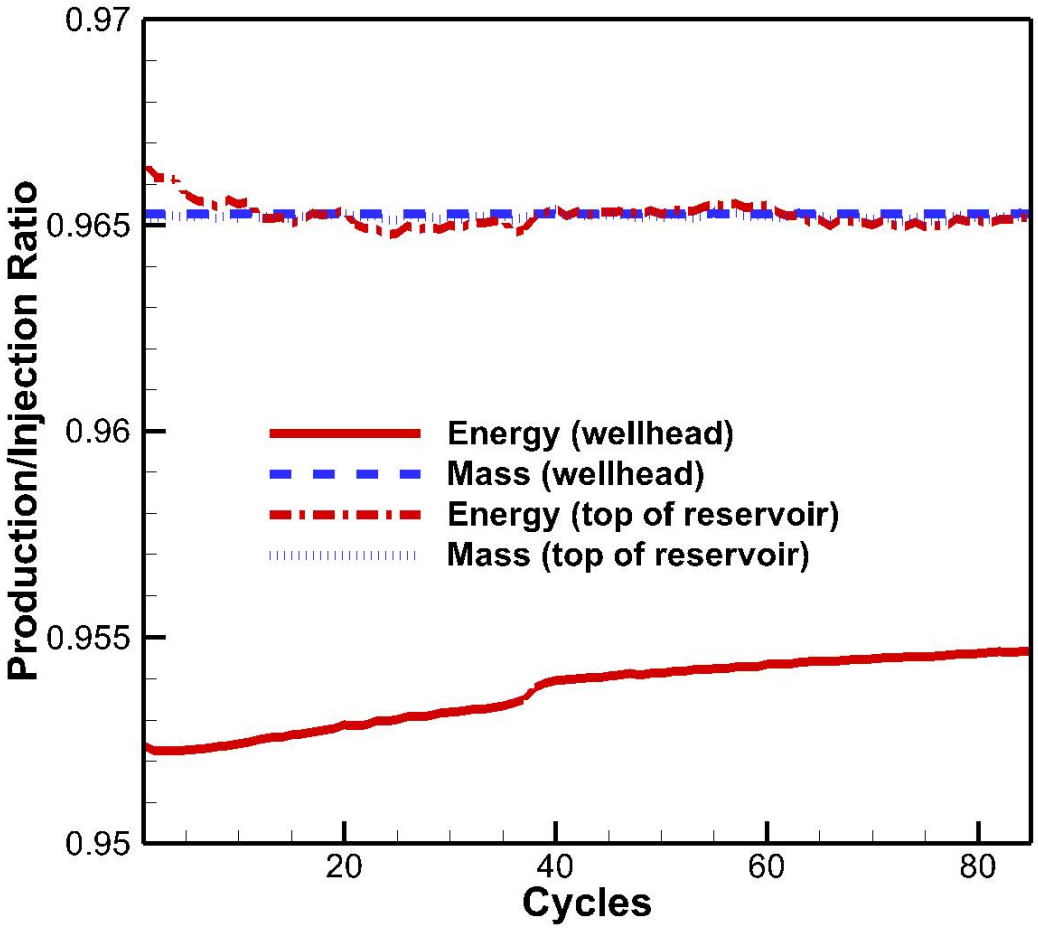

Figure 7. Efficiency of mass and energy flows in the wellbore-reservoir PM-CAES system at the wellhead and in the well at the top of the reservoir.

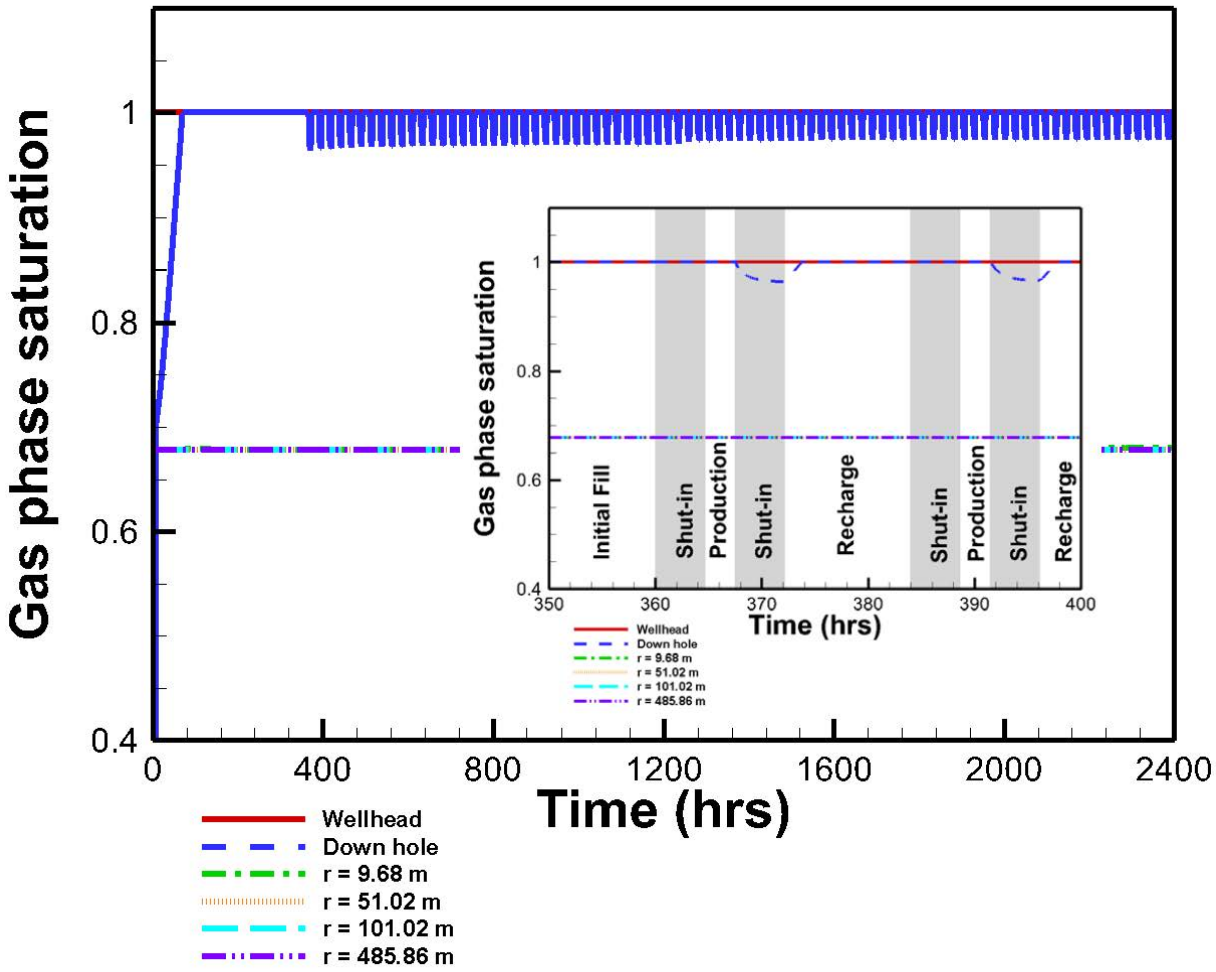

Figure 8. Gas-phase saturation at six different locations in the reservoir during initial fill of air and over 100 daily cycles, and over two cycles (inset) to show detail. The results at various values of r (radius from well) are at the midpoint of thickness in the reservoir.